Molecular Therapy
Nucleic Acids
Original Article

miR-455-3p Alleviates Hepatic Stellate Cell Activation and Liver Fibrosis by Suppressing HSF1 Expression

Song Wei,[1,4] Qi Wang,[2,4] Haoming Zhou,[2] Jiannan Qiu,[2] Changyong Li,[3] Chengyu Shi,[2] Shun Zhou,[2] Rui Liu,[2] and Ling Lu[1,2]

[1]School of Medicine, Southeast University, Nanjing 210009, China; [2]Liver Transplantation Center, The First Affiliated Hospital of Nanjing Medical University, Nanjing, China; [3]Department of Physiology, School of Basic Medical Sciences, Wuhan University, Wuhan, China

Liver fibrosis is a common pathological process of end-stage liver diseases. However, the role of microRNA (miRNA) in liver fibrosis is poorly understood. The activated hepatic stellate cells (HSCs) are the major source of fibrogenic cells and play a central role in liver fibrosis. In this study, we investigated the differential expression of miRNAs in resting and transforming growth factor β1 (TGF-β1) activated HSCs by microarray analysis and found that miR-455-3p was significantly downregulated during HSCs activation. In addition, the reduction of miR-455-3p was correlated with liver fibrosis in mice with carbon tetrachloride (CCl_4), bile duct ligation (BDL), and high-fat diet (HFD)-induced liver fibrosis. Our functional analyses demonstrated that miR-455-3p inhibited expression of profibrotic markers and cell proliferation in HSCs *in vitro*. Moreover, miR-455-3p regulated heat shock factor 1 (HSF1) expression by binding to the 3′ UTR of its mRNA directly. Overexpression of HSF1 facilitated HSCs activation and proliferation by promoting heat shock protein 47 (Hsp47) expression, leading to activation of the TGF-β/Smad4 signaling pathway. To explore the clinical potential of miR-455-3p, we injected ago-miR-455-3p into mice with CCl_4-, BDL-, and HFD-induced hepatic fibrosis *in vivo*. The overexpression of miR-455-3p suppressed HSF1 expression and reduced fibrosis marker expression, which resulted in alleviated liver fibrosis in mice. In conclusion, our present study suggests that miR-455-3p inhibits the activation of HSCs through targeting HSF1 involved in the Hsp47/TGF-β/Smad4 signaling pathway. Therefore, miR-455-3p might be a promising therapeutic target for liver fibrosis.

INTRODUCTION

Liver fibrosis is a common pathological process of end-stage liver diseases. Advanced fibrosis leads to cirrhosis, liver failure, hepatocarcinoma, and ultimately death.[1] The development of fibrosis is connected with a sustained wound-healing process in response to liver injury, characterized by increased production of matrix proteins and decreased matrix remodeling.[2] Hepatic stellate cells (HSCs) are considered the fibrogenic cell type in the liver.[3] In the injured liver, activated HSCs are the main producer of extracellular matrix.[4] The activation of HSCs is controlled by multiple soluble mediators including transforming growth factor β (TGF-β) and platelet-derived growth factor (PDGF).[5,6] However, the mechanisms of HSC activation in liver fibrosis remain largely elusive.

MicroRNAs (miRNAs), a class of small noncoding RNAs composed of ~22–25 nt, function as post-transcriptional regulators by inducing degradation of mRNAs of target genes.[7] Recent studies have shown the effect of miRNAs on HSCs activation and transformation, which is essential for the pathogenesis of liver fibrosis.[8] For example, miR-185 inhibits fibrogenic activation of HSCs and prevents liver fibrosis.[9] miR-30a ameliorates hepatic fibrosis by inhibiting Beclin1-mediated autophagy.[10] miR-122 regulates collagen production via targeting HSCs and suppressing P4HA1 expression.[11] miR-214 promotes HSC activation and liver fibrosis by suppressing Sufu expression.[12] However, the underlying mechanisms by which miRNAs regulate HSC activation are still largely unknown. Therefore, investigating how miRNAs are involved in HSC activation may promote the discovery of new therapeutic targets and efficacious treatment strategies for hepatic fibrosis.

In this study, we investigated the function and molecular mechanisms of miR-455-3p in hepatic fibrosis. First, we compared miRNA expression profiles between resting and activated HSCs. Our results showed that miR-455-3p was downregulated in activated HSCs induced by TGF-β1. These findings were subsequently verified in animal models. Moreover, overexpression of miR-455-3p inhibited expression of profibrotic markers and cell proliferation in HSCs *in vitro*. Mechanistically, miR-455-3p regulated HSF1 expression by binding to the 3′ UTR of its mRNA directly. Importantly, *in vivo* administration of ago-miR-455-3p alleviated

Received 14 December 2018; accepted 2 May 2019;
https://doi.org/10.1016/j.omtn.2019.05.001.

[4]These authors contributed equally to this work.

Correspondence: Ling Lu, School of Medicine, Southeast University, 87 Ding Jia Qiao Road, Nanjing 210009, China.
E-mail: lvling@njmu.edu.cn

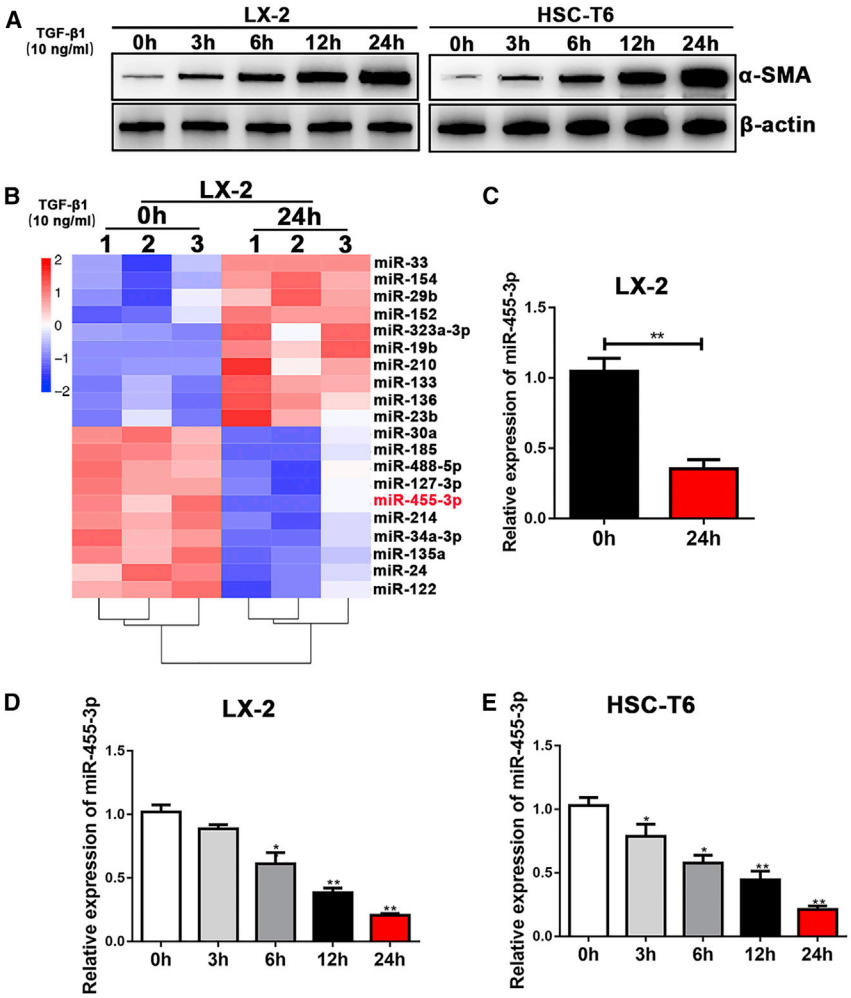

Figure 1. miR-455-3p Is Downregulated in Activated HSCs Induced by TGF-β1

(A) The protein level of α-SMA was upregulated in activated LX-2 and HSC-T6 cells treated with 10 ng/mL TGF-β1 in a time-dependent manner. (B) Microarray analysis for miRNA expression was performed using total RNAs extracted from resting and activated LX-2 cells. (C) The expression level of miR-455-3p in LX-2 cells was examined by quantitative real-time PCR. (D and E) The expression level of miR-455-3p in activated (D) LX-2 cells and (E) HSC-T6 cells was examined in a time-dependent manner. Graph represents mean ± SEM. *$p < 0.05$, **$p < 0.01$, and ***$p < 0.001$.

hepatic fibrosis in mice. In general, our findings revealed that miR-455-3p plays a pivotal role in liver fibrosis by regulating HSF1 signaling, and it may be used as a potential therapeutic target.

RESULTS

miR-455-3p Is Downregulated in Activated HSCs Induced by TGF-β1

We detected the expression levels of α-smooth muscle actin (α-SMA) in activated HSCs induced by TGF-β1 first; the expression level of α-SMA was upregulated in a time-dependent manner in both LX-2 and HSC-T6 cells. In addition, we found that the expression of α-SMA was highest in LX-2 and HSC-T6 cells added to 10 ng/mL TGF-β1 for 24 h (Figure 1A). To explore the changes in miRNA expression profiles after HSC activation, we performed miRNA microarray analysis on total RNAs extracted from LX-2 added to 10 ng/mL TGF-β1 for 0 and 24 h. As shown in Figure 1B, 20 miRNAs were significantly differently expressed after TGF-β1-induced LX-2 activation. We found that miR-455-3p was one of the most significantly downregulated miRNAs. Quantitative real-time PCR analysis was used to further validate its downregulation (Figure 1C). In addition, miR-455-3p level showed a time-dependent decrease in response to TGF-β1 in LX-2 and HSC-T6 cells (Figures 1D and 1E). In conclusion, our results indicated a downregulated expression of miR-455-3p in activated HSCs induced by TGF-β1.

miR-455-3p Is Downregulated in Different Hepatic Fibrosis Models

Next, mice were subjected to carbon tetrachloride (CCl_4) or bile duct ligation (BDL) to develop different hepatic fibrosis models. The results of H&E and Masson staining revealed the increased liver fibrosis and collagen deposition in mice after CCl_4 and BDL treatment (Figures 2A and 2B). It has been recognized that non-alcoholic steatohepatitis (NASH) is a major cause of liver fibrosis, so we induced NASH in mice by feeding the mice a high-fat diet (HFD). Consistent with the results of mice after CCl_4 and BDL treatment, advanced liver fibrosis was found in mice with HFD-induced liver fibrosis (Figures 2C and 2D). The mRNA levels of fibrotic genes, including α-SMA, Collagen-I, and tissue inhibitor of metalloproteinases 1 (TIMP-1), were higher in the livers of CCl_4-, BDL-, and HFD-treated mice than those of control (Figures 2E–2G). Moreover, compared with that in the control mice, miR-455-3p expression was significantly decreased in the liver of mice with CCl_4-, BDL-, and HFD-induced liver fibrosis (Figure 2H). These observations indicated that miR-455-3p played a crucial role in the progression of liver fibrosis.

Overexpression of miR-455-3p Inhibits Expression of Profibrotic Markers and Cell Proliferation in HSCs

To explore the functional role of miR-455-3p in hepatic fibrosis, LX-2 and HSC-T6 cells were transfected with miR-455-3p mimics. The miR-455-3p levels were significantly higher in LX-2 and HSC-T6 cells after transfection with miR-455-3p mimics (Figure 3A). The protein levels of profibrotic markers, including α-SMA, Collagen-I, and TIMP-1, were significantly repressed following the overexpression of miR-455-3p in LX-2 and HSC-T6 cells (Figure 3B). In addition,

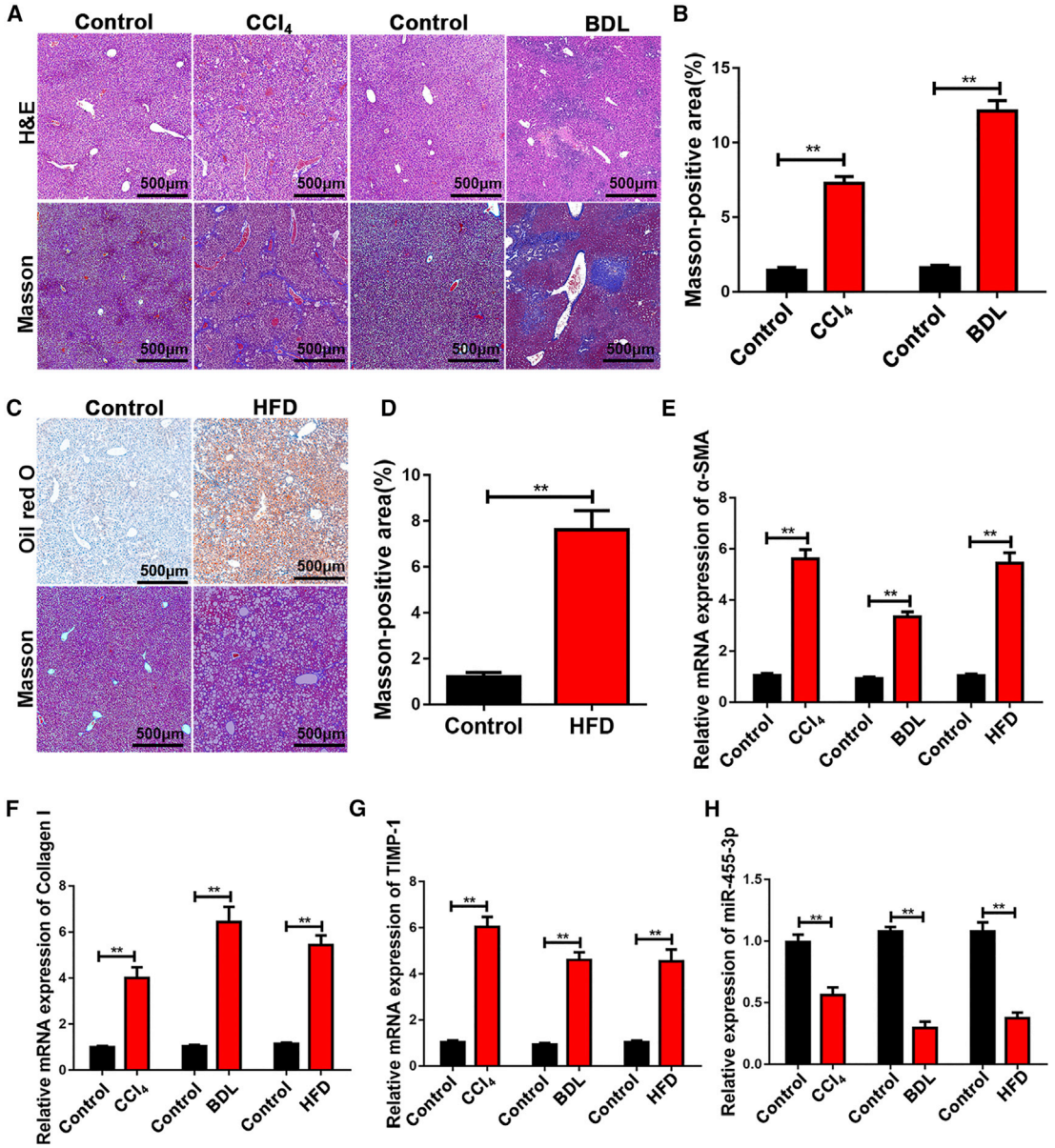

Figure 2. miR-455-3p Is Downregulated in Different Hepatic Fibrosis Models

(A) Representative images of H&E and Masson staining of liver sections in mice exposed to CCl_4 for 8 weeks and BDL for 2 weeks (original magnification ×50; scale bars, 500 μm). (B) The quantification of Masson-positive fibrosis areas in mice exposed to CCl_4 for 8 weeks and BDL for 2 weeks. (C) Representative images of oil red staining and Masson staining of liver sections in mice with HFD for 24 weeks (original magnification ×50; scale bars, 500 μm). (D) The quantification of Masson-positive fibrosis areas in mice with HFD-induced liver fibrosis. (E) The expression level of α-SMA was examined in the mice with CCl_4-, BDL-, and HFD-induced liver fibrosis by quantitative real-time PCR. (F) The expression level of Collagen-I was examined in the mice with CCl_4-, BDL-, and HFD-induced liver fibrosis by quantitative real-time PCR. (G) The expression level of TIMP-1 was examined in the mice with CCl_4-, BDL-, and HFD-induced liver fibrosis by quantitative real-time PCR. (H) The expression level of miR-455-3p was examined in the mice with CCl_4-, BDL-, and HFD-induced liver fibrosis by quantitative real-time PCR. Graph represents mean ± SEM. *$p < 0.05$, **$p < 0.01$, and ***$p < 0.001$.

overexpression of miR-455-3p also significantly inhibited cell growth in both LX-2 and HSC-T6 cells (Figure 3C). Next, we investigated whether miR-455-3p affected the cell cycle of HSCs. As determined by cell-cycle assay, overexpression of miR-455-3p significantly reduced the percentage of cells in S phase, indicating miR-455-3p could influence cell-cycle distribution in HSCs (Figures 3D and 3E). Moreover, overexpression of miR-455-3p also led to increased apoptosis in LX-2 and HSC-T6 cells (Figures 3F and 3G). Our finding revealed that overexpression of miR-455-3p could inhibit expression of profibrotic markers and cell proliferation in HSCs.

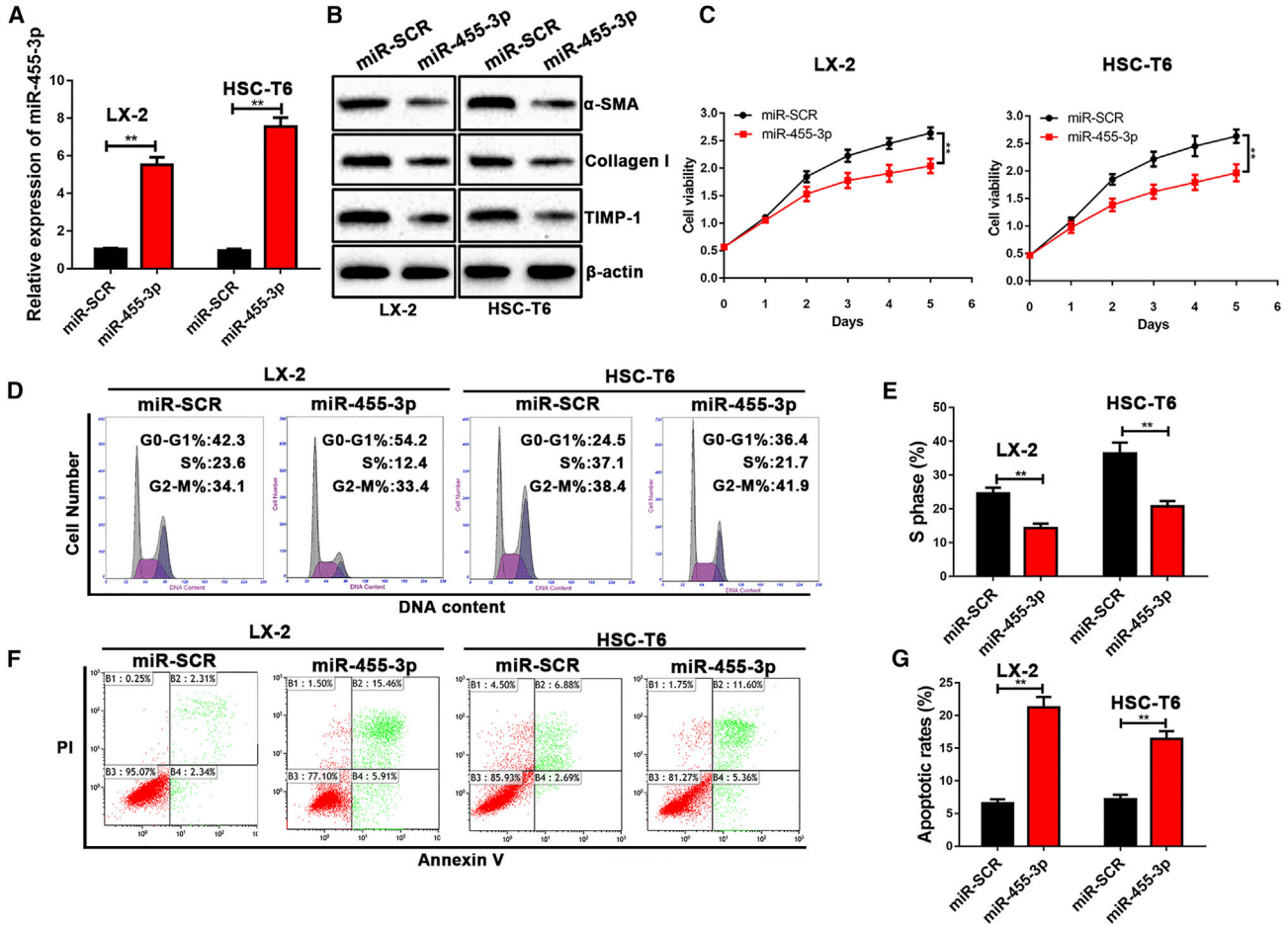

Figure 3. Overexpression of miR-455-3p Inhibits Expression of Profibrotic Markers and Cell Proliferation in HSCs

(A) The expression level of miR-455-3p was examined in LX-2 and HSC-T6 cells after transfection with miR-455-3p mimics. (B) The protein levels of α-SMA, Collagen-I, and TIMP-1 were examined by western blotting. (C) Proliferation of LX-2 and HSC-T6 cells transfected with miR-SCR and miR-455-3p was detected by cell viability assay. (D) The cell-cycle distribution of miR-455-3p-overexpressed LX-2 and HSC-T6 cells was detected by flow cytometry and (E) the quantification. (F) The cell apoptosis of miR-455-3p-overexpressed LX-2 and HSC-T6 cells was detected by flow cytometry and (G) the quantification. Graph represents mean ± SEM. *$p < 0.05$, **$p < 0.01$, and ***$p < 0.001$.

miR-455-3p Regulates HSF1 Expression by Binding to the 3′ UTR of Its mRNA Directly

To identify the mechanism how miR-455-3p regulates HSC activation, we performed bioinformatics analyses with software including miRbase, miRanda, and TargetScan. We found that HSF1 could be a potential target gene of miR-455-3p (Figure 4A). It has been reported that inactivation of HSF1 could suppress collagen production in HSCs.[13] However, whether miR-455-3p regulates HSF1 expression in HSCs and in liver fibrosis models has not yet been examined. We transfected miR-455-3p mimics into LX-2 and HSC-T6 cells. As shown in Figure 4B, overexpression of miR-455-3p decreased the expression of HSF1 in LX-2 and HSC-T6 cells. Luciferase reporter gene assay was used to verify the direct interaction between miR-455-3p and HSF1. Wild-type (WT) or MUT 3′ UTR target sequences were cloned into a luciferase reporter vector. Luciferase activity of WT 3′ UTR of HSF1 was significantly inhibited by miR-455-3p in LX-2 and HSC-T6 cells (Figure 4C). To examine the role of HSF1 in liver fibrosis, we detected the protein expression of HSF1 in LX-2 and HSC-T6 cells activated by TGF-β1. We found that the protein expression of HSF1 was increased in activated LX-2 and HSC-T6 cells (Figure 4D). In addition, the expression levels of HSF1 were higher in the livers of CCl_4-, BDL-, and HFD-treated mice than those of control (Figure 4E). Moreover, the results of western blotting revealed that the expression level of HSF1 was significantly higher in liver tissues of patients with liver fibrosis than those in heathy controls (Figure 4F). We further examined the expression of HSF1 using immunochemistry. Consistent with the result of western blotting, the expression of HSF1 was increased in liver tissues from patients with liver fibrosis (Figure 4G). As shown in Figure 4H, overexpression of miR-455-3p could decrease the expression levels of HSF1, heat shock protein 47 (Hsp47),

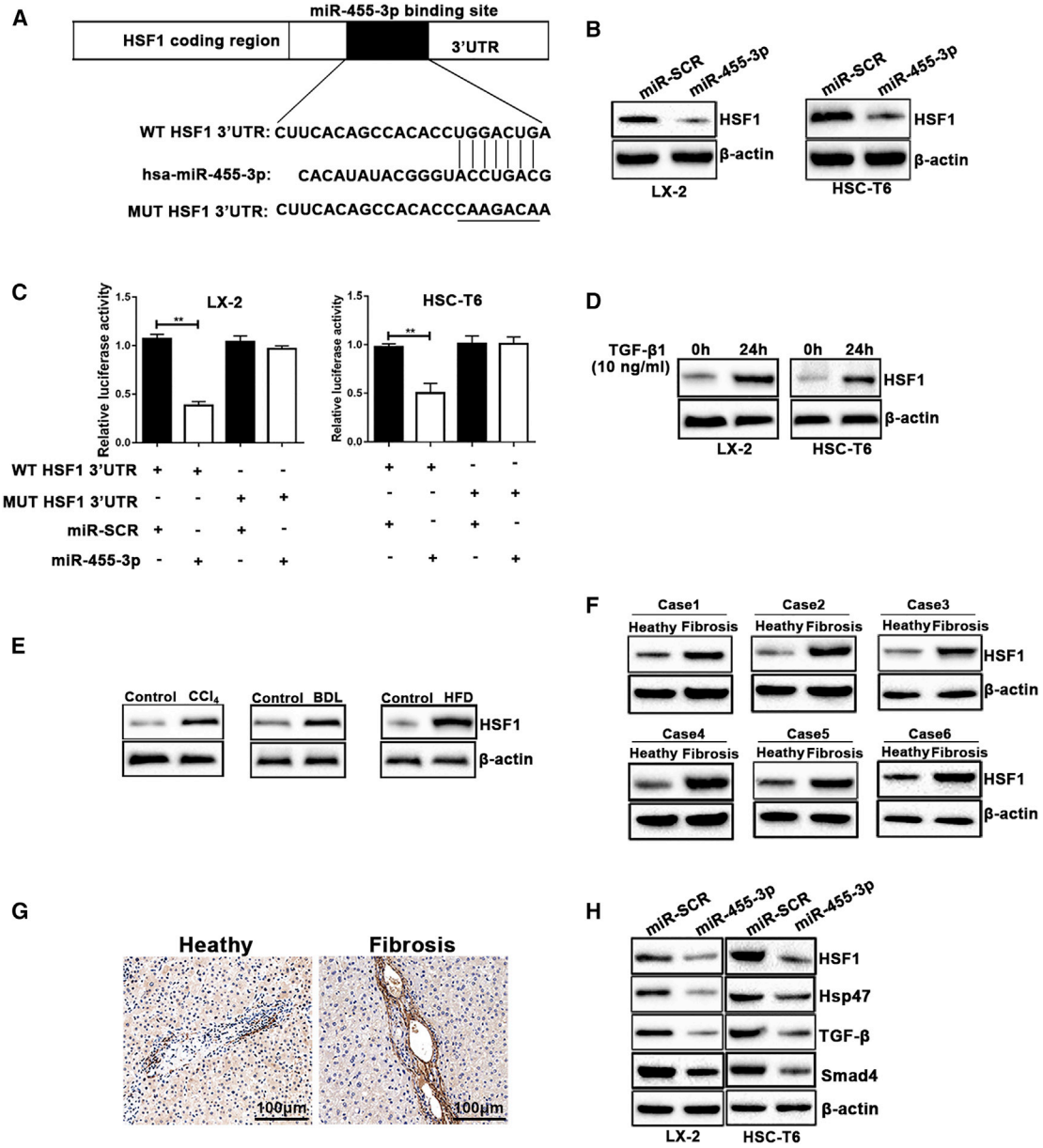

Figure 4. miR-455-3p Regulates HSF1 Expression by Binding to the 3′ UTR of Its mRNA Directly

(A) Predicted miR-455-3p targeting sequence in HSF1 3′ UTR (WT HSF1 3′ UTR). Target sequences of HSF1 3′ UTR were mutated (MUT HSF1 3′ UTR). (B) The protein levels of HSF1 were examined by western blotting. (C) Dual-luciferase reporter assay of LX-2 and HSC-T6 cells transfected with WT HSF1 3′ UTR or MUT HSF1 3′UTR reporter together with 40 nM miR-455-3p mimics or negative control oligoribonucleotides. (D) The protein levels of HSF1 in LX-2 and HSC-T6 cells treated with 10 ng/mL TGF-β1 for 0 and 24 h. (E) The expression level of HSF1 was examined in the mice with CCl_4-, BDL-, and HFD-induced liver fibrosis by western blotting. (F) The protein levels of HSF1 were examined in liver tissues from healthy controls or patients with liver fibrosis. (G) Immunohistochemical staining of HSF1 in liver tissues from healthy controls or patients with liver fibrosis (original magnification ×200; scale bars, 100 μm). (H) The protein levels of HSF1, Hsp47, TGF-β, and Smad4 were examined by western blotting. Graph represents mean ± SEM. *$p < 0.05$, **$p < 0.01$, and ***$p < 0.001$.

TGF-β, and smad4. These results indicated that HSF1 might be a target gene of miR-455-3p in LX-2 and HSC-T6 cells, which were involved in the Hsp47/TGF-β/Smad4 signaling pathway in HSCs and liver fibrosis.

miR-455-3p-Mediated HSC Activation and Proliferation Depend on HSF1 Expression

To further elucidate that miR-455-3p regulated HSC activation and proliferation by targeting HSF1, we used lentivirus to overexpress HSF1 in

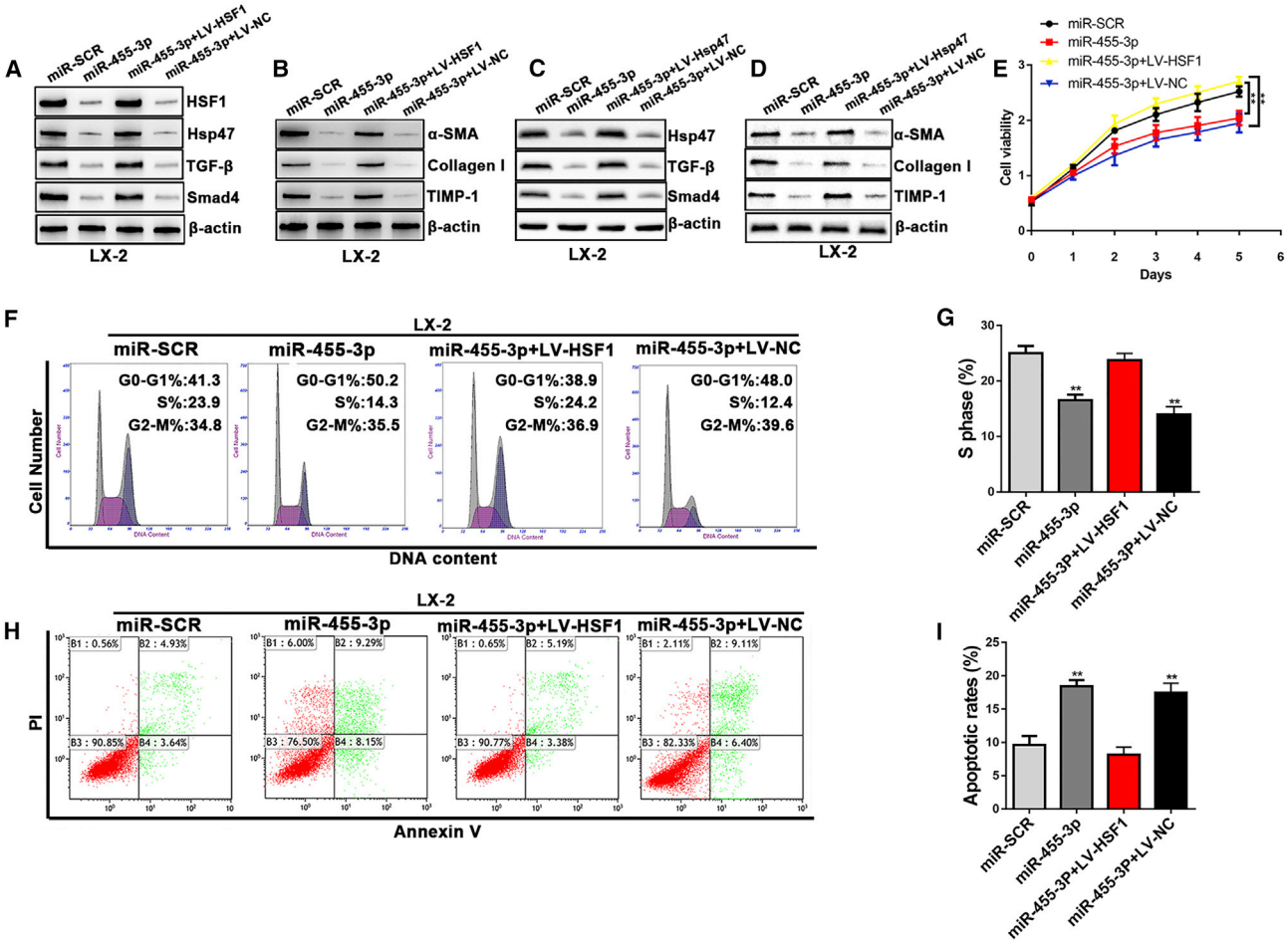

Figure 5. miR-455-3p-Mediated HSC Activation and Proliferation Depend on HSF1 Expression

(A) The expression levels of HSF1, Hsp47, TGF-β, and Smad4 were examined in LX-2-pre-miR-455-3p cells transfected with LV-HSF1 or LV-NC. (B) The protein levels of α-SMA, Collagen-I, and TIMP-1 were examined by western blotting in LX-2-pre-miR-455-3p cells transfected with LV-HSF1 or LV-NC. (C) The expression levels of Hsp47, TGF-β, and Smad4 were examined in LX-2-pre-miR-455-3p cells transfected with LV-Hsp47 or LV-NC. (D) The protein levels of α-SMA, Collagen-I, and TIMP-1 were examined by western blotting in LX-2-pre-miR-455-3p cells transfected with LV-Hsp47 or LV-NC. (E) Proliferation of LX-2-pre-miR-455-3p cells transfected with LV-HSF1 or LV-NC was detected by cell viability assay. (F) The cell-cycle distribution of LX-2-pre-miR-455-3p cells transfected with LV-HSF1 or LV-NC was detected by flow cytometry and (G) the quantification. (H) The cell apoptosis of LX-2-pre-miR-455-3p cells transfected with LV-HSF1 or LV-NC was detected by flow cytometry and (I) the quantification. Graph represents mean ± SEM. *$p < 0.05$, **$p < 0.01$, and ***$p < 0.001$.

LX-2 cells transfected with miR-455-3p mimics. Overexpression of HSF1 resulted in upregulation of HSF1, Hsp47, TGF-β, and Smad4 in LX-2 transfected with miR-455-3p mimics (Figure 5A). Moreover, when HSF1 expression was overexpressed in LX-2 cells that were transfected with miR-455-3p mimics, the expression of profibrotic markers including α-SMA, Collagen-I, and TIMP-1 was significantly upregulated (Figure 5B). To explore the role of Hsp47 in miR-455-3p-mediated HSC activation, Hsp47 lentivirus was used to overexpress Hsp47 in LX-2 cells transfected with miR-455-3p mimics and control. The expression levels of TGF-β and Smad4 were significantly higher in LX-2 cells transfected with Hsp47 lentivirus compared with control (Figure 5C). In addition, overexpression of Hsp47 could increase the expression level of α-SMA, Collagen-I, and TIMP-1 in LX-2 cells transfected with miR-455-3p mimics compared with control (Figure 5D). As shown in Figure 5E, overexpression of HSF1 significantly reversed the inhibitory effects of miR-455-3p on HSC proliferation according to the results of the cell viability assay. In addition, HSF1 overexpression reversed the S phase arrest in LX-2 cells transfected with miR-455-3p mimics (Figures 5F and 5G). Similarly, the effects of miR-455-3p on LX-2 and HSC-T6 cell apoptosis were counteracted by HSF1 overexpression (Figures 5H and 5I). These findings demonstrated that the miR-455-3p/HSF1 axis played an important role in regulating HSC activation and proliferation.

miR-455-3p Prevents Hepatic Fibrosis in Mice

According to our results, miR-455-3p regulated HSC activation and proliferation *in vitro*. To further investigate the role of miR-455-3p

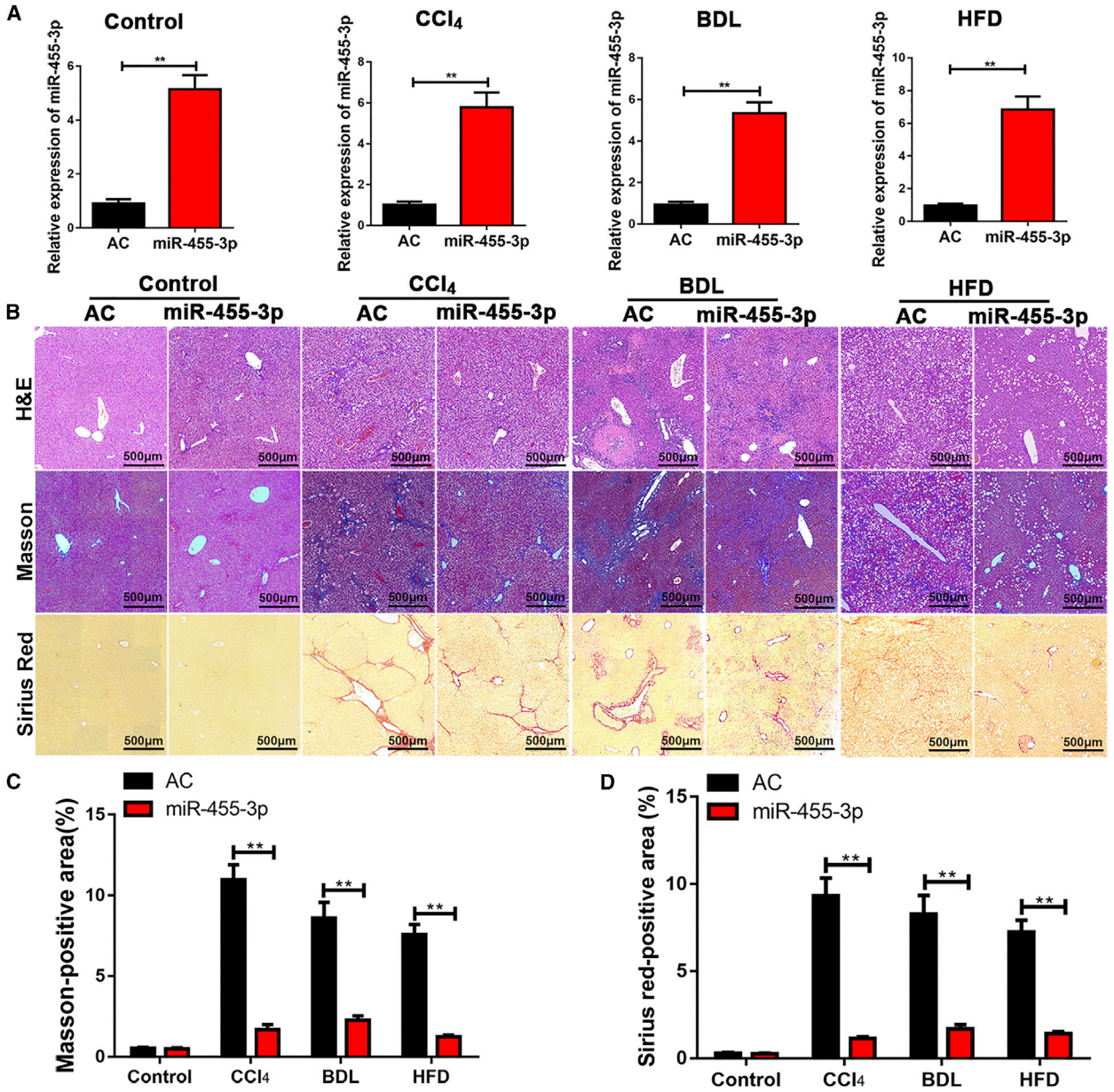

Figure 6. miR-455-3p Prevents Hepatic Fibrosis in Mice

(A) The expression level of miR-455-3p was examined in mice transfected with AC and ago-miR-455-3p. (B) Representative images of H&E, Masson, and Sirius red staining of liver sections in untreated mice and mice with CCl_4-, BDL-, and HFD-induced liver fibrosis (original magnification ×50; scale bars, 500 μm). (C) The quantification of Masson-positive fibrosis areas. (D) The quantification of Sirius red-positive fibrosis areas. Graph represents mean ± SEM. *$p < 0.05$, **$p < 0.01$, and ***$p < 0.001$.

in hepatic fibrosis *in vivo*, the Agomir control (AC) and ago-miR-455-3p were transfected into untreated mice and mice with CCl_4-, BDL-, and HFD-induced liver fibrosis. The level of miR-455-3p in liver tissues was detected by quantitative real-time PCR (Figure 6A). H&E, Masson, and Sirius staining demonstrated that overexpression of miR-455-3p alleviated hepatic fibrosis *in vivo* (Figures 6B–6D). Collectively, these findings indicated that miR-455-3p could prevent hepatic fibrosis in different hepatic fibrosis models.

miR-455-3p Suppresses HSF1 Expression in Hepatic Fibrosis Tissues

We found that overexpression of miR-455-3p inhibited the α-SMA expression in mice with CCl_4-, BDL-, and HFD-induced liver fibrosis, which was detected by immunohistochemistry. There was no significant difference in untreated mice transfected with AC and ago-miR-455-3p (Figures 7A and 7B). We also determined the protein level of profibrotic markers including α-SMA, Collagen-I, and

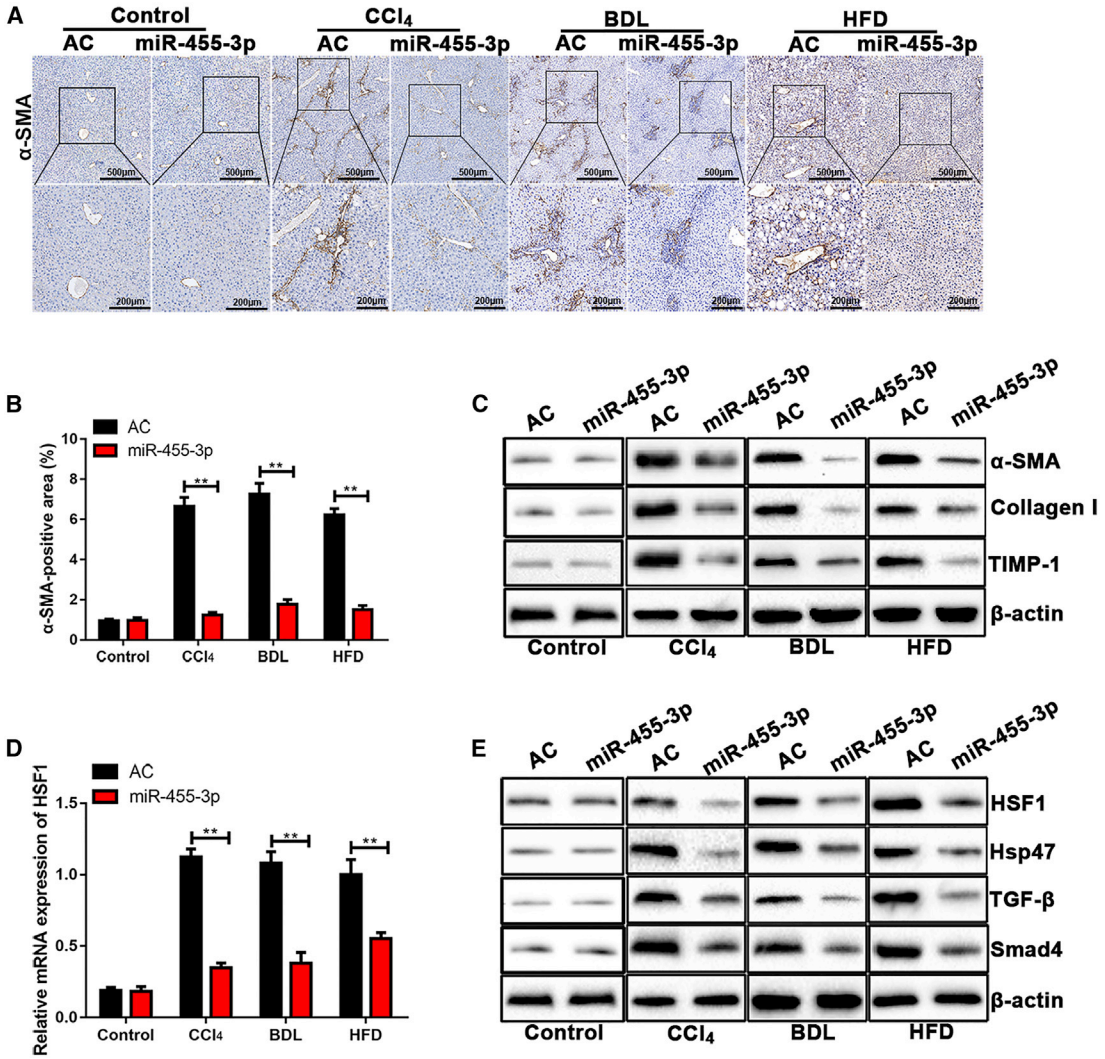

Figure 7. miR-455-3p Suppresses HSF1 Expression in Hepatic Fibrosis Tissues

(A) Immunohistochemical staining of α-SMA in liver tissues from mice transfected with the AC and ago-miR-455-3p with CCl_4-, BDL-, and HFD-induced liver fibrosis. (B) The quantification of the α-SMA-positive area in untreated mice and mice transfected with the AC and ago-miR-455-3p with CCl_4-, BDL-, and HFD-induced liver fibrosis. (C) The protein levels of α-SMA, Collagen-I, and TIMP-1 in liver tissues from untreated mice and mice transfected with the AC and ago-miR-455-3p with CCl_4-, BDL-, and HFD-induced liver fibrosis were examined by western blotting. (D) The expression level of HSF1 in untreated mice and mice transfected with AC and ago-miR-455-3p with CCl_4-, BDL-, and HFD-induced liver fibrosis was examined by quantitative real-time PCR. (E) The protein levels of HSF1, Hsp47, TGF-β, and Smad4 in liver tissues from untreated mice and mice transfected with AC and ago-miR-455-3p with CCl_4-, BDL-, and HFD-induced liver fibrosis were examined by western blotting. Graph represents mean ± SEM. *$p < 0.05$, **$p < 0.01$, and ***$p < 0.001$.

TIMP-1 in liver tissues from mice transfected with AC and ago-miR-455-3p. The expression levels of α-SMA, Collagen-I, and TIMP-1 were significantly lower in CCl_4-, BDL-, and HFD-treated mice transfected with ago-miR-455-3p compared with control. Overexpression of miR-455-3p did not change the expression levels of α-SMA, Collagen-I, and TIMP-1 in the untreated group transfected with AC and ago-miR-455-3p (Figure 7C). To identify whether miR-455-3p could regulate HSF1 expression in the hepatic fibrosis model, we examined the expression level of HSF1 using quantitative real-time PCR. As shown in Figure 7D, a significantly lower expression level of HSF1 was found in CCl_4-, BDL-, and HFD-treated mice transfected with ago-miR-455-3p compared with control. However, the expression level of HSF1 was unchanged in untreated mice transfected with AC and ago-miR-455-3p. In addition, we found that miR-455-3p overexpression reduced the expression levels of HSF1, Hsp47, TGF-β, and Smad4 in liver of CCl_4-, BDL-, and HFD-treated mice after treatment with ago-miR-455-3p compared with control. There was no significant difference in the expression level of HSF1, Hsp47, TGF-β, and Smad4 in untreated mice transfected with AC and ago-miR-455-3p (Figure 7E). Collectively, our

findings revealed that miR-455-3p alleviated hepatic fibrosis through targeting HSF1 by the Hsp47/TGF-β/Smad4 signaling pathway.

DISCUSSION

Liver fibrosis is a chronic disease caused by viral infection, alcohol abuse, and metabolic and genetic disorders, which leads to an excessive accumulation of extracellular matrix proteins.[14] HSCs have been recognized as the major source of extracellular matrix.[15] HSC activation and trans-differentiation into myofibroblasts are believed to be the key events in the process of liver fibrosis.[16]

In recent years, researchers have focused on the role of miRNAs in the pathophysiology of hepatic fibrosis to determine its role in the regulation of HSC proliferation and differentiation.[17] Aberrant expression of several miRNAs was identified between resting and activated HSCs.[18] A recent study shows that miR-455-3p served as oncogene or anti-oncogene in different types of tumors.[19] Several reports have demonstrated that miR-455-3p participated in fibrosis.[20] For example, miR-455-3p suppressed renal fibrosis through repression of ROCK2 expression.[21] However, it remains unclear whether miR-455-3p was involved in HSC activation that resulted in liver fibrosis.

In this study, we found that miR-455-3p was downregulated in activated HSCs induced by TGF-β1 using microarray analysis *in vitro*. *In vivo*, we developed three different hepatic fibrosis models, including CCl_4, BDL, and HFD. We found that miR-455-3p was downregulated in different hepatic fibrosis models, which was in accordance with the results in activated HSCs. Our findings suggested that miR-455-3p might play an inhibiting role in liver fibrogenesis, and its downregulation might be associated with the HSC activation.

According to the bioinformatics analyses results, we found that HSF1 might be the direct targeting gene of miR-455-3p. HSF1 is the transcription factor primarily responsible for the transcriptional response of cells to physical and chemical stress, which assist in refolding or degrading damaged proteins.[22,23] HSF1 activation is accomplished at the post-translational modification and protein-protein interaction level.[24] In recent years, HSF1 has been revealed to regulate some cellular behaviors, such as apoptosis and proliferation.[25] According to our study, miR-455-3p could regulate HSF1 expression by binding to the 3′ UTR of its mRNA directly. We also found that overexpression of HSF1 upregulated expression of Hsp47 in HSCs transfected with miR-455-3p. It has been reported that ROCK2 is involved in miR-455-3p-meditated renal fibrosis.[26] It is possible that ROCK2 is also important in liver fibrosis. Whether ROCK2 is involved in miR-455-3p-meditated liver fibrosis needs to be further studied. Hsp47 is a collagen-specific molecular that contributes to molecular maturation of collagen.[13] It has been reported that Hsp47 plays an important role in collagen synthesis.[27] In lung fibrosis, Hsp47-positive cells are the main source of collagen synthesis.[28] A recent study shows that induction of Hsp47 synthesis was regulated through activation of HSF1.[29] Downregulation of Hsp47 by HSF1 inhibition might delay or diminish the progression of fibrosis by reducing the accumulation of collagens.[30] Overexpression of Hsp47 was correlated and promoted extracellular matrix-related genes through the TGF-β pathway.[31] TGF-β is a cytokine that is related to many biological activities, including cell proliferation, differentiation, migration, and apoptosis.[32] In addition, the TGF-β signaling pathway plays a major role in the activation of HSCs.[33] TGF-β performs its profibrotic effects via cascade stimulation of downstream intracellular Smad proteins.[34] Smad2, Smad3, and Smad4 are necessary for TGF-β signal transduction among these Smads.[35] In the context of hepatic fibrosis, Smad3 and Smad4 are pro-fibrotic, whereas Smad3 and Smad7 are protective.[36] In our study, we found that miR-455-3p could alleviate HSC activation and liver fibrosis by targeting HSF1 through inhibiting the Hsp47/TGF-β/Smad4 signaling pathway.

In summary, our study demonstrated that miR-455-3p was downregulated both in activated HSCs and different hepatic fibrosis models. Overexpression of miR-455-3p inhibited expression of profibrotic markers and cell proliferation in HSCs by targeting HSF1 through inhibiting the Hsp47/TGF-β/Smad4 signaling pathway. Moreover, miR-455-3p prevented hepatic fibrosis and suppressed HSF1 expression in mice. Our findings provided new insights into the cellular mechanisms by which the miR-455-3p alleviated liver fibrosis by regulating the HSF1 signaling pathway.

MATERIALS AND METHODS

Patient Samples

Liver tissues were obtained from patients who underwent liver resection in the first Affiliated Hospital of Nanjing Medical University. The tissues were rapidly frozen in liquid nitrogen following surgical resection. Samples from patients with different stages of liver fibrosis were analyzed according to the Meta-analysis of Histological Data in Viral Hepatitis (METAVIR) score. All specimens were collected upon obtaining informed consent from all patients. All procedures that involved human samples were approved by the Ethics Committee of the Affiliated Hospital of Nanjing Medical University.

HSCs Activated by TGF-β1

HSC-T6 and LX-2 cells were purchased from the Cell Center of Shanghai Institutes for Biological Sciences. Cells were cultured in DMEM (Sigma-Aldrich, St. Louis, MO, USA) containing 10% fetal bovine serum (FBS; WISENT, Canada). HSC-T6 and LX-2 cells were treated with TGF-β1 (10 ng/mL) for 0, 3, 6, 12, and 24 h in DMEM without serum, respectively, for activation.

Western Blotting

Western blot was performed routinely, with primary antibodies against α-SMA, Collagen-I, TIMP-1, TGF-β, Smad4, β-actin (1:1,000; Cell Signaling Technology), and HSF1 (1:200; Santa Cruz Biotechnology). HRP-conjugated goat anti-rabbit immunoglobulin G (IgG) or goat anti-mouse IgG (1:1,000; Cell Signaling Technology) was used as the secondary antibody. The signals were detected using the Chemiluminescence HRP Substrate (WBKL0100; Millipore) and an enhanced chemiluminescence detection system.

Quantitative Real-Time PCR

The levels of U6 and miR-455-3p were tested using the TaqMan miRNA assay system (Life Technologies Corporation, Shanghai, China). To detect mRNA expression, total RNA was isolated using TRIzol reagent (Invitrogen, Carlsbad, CA, USA) and was reverse transcribed into cDNA using the Transcriptor First Strand cDNA Synthesis Kit (Roche, Indianapolis, IN, USA). Quantitative real-time PCR was performed using SYBR green (Life Technologies, Grand Island, NY, USA). The expression levels of target genes and the results were normalized against β-actin expression. The primers used in this study were as follows: Has-miR-455-3p, forward: 5′-GCAGTCCATGGGCATATACAC-3′; U6, forward: 5′-CTCGCT TCGGCAGCACA-3′; HSF1, forward: 5′-CCTGGTCAAGCCAGA GAGAG-3′, reverse: 5′-CTGCACCAGTGAGATCAGGA-3′; α-SMA, forward: 5′-GGCTCTGGGCTCTGTAAGG-3′, reverse: 5′-CTCTTG CTCTGGGCTTCAT; C-3′; Collagen-I, forward: 5′-GCTCCTCTT AGGGGCCACT-3′, reverse: 5′-CCACGTCTCACCATT; GGGG-3′; TIMP-1, forward: 5′-GCAACTCGGACCTGGTCATAA-3′, reverse: 5′-CGGCCCGTGAT; GAGAAACT-3′; β-actin, forward: 5′-CTAAG GCCAACCGTGAAAAG-3′, reverse: 5′-ACCAGAGGCATACAGG GACA-3′.

miR-455-3p and HSF1 Transfection *In Vitro or In Vivo*

The scrambled miRNA served as negative control (miR-SCR); miR-455-3p-mimics, HSF1 Lentivirus (LV-HSF1) and negative control, and Hsp47 Lentivirus (LV-Hsp47) and negative control were purchased from GenePharma (Shanghai, China). Lentivirus were transfected into HSC-T6 and LX-2 cells using Lipofectamine 2000 (Invitrogen, Carlsbad, CA, USA). AC and ago-miR-455-3p (Gema, Shanghai, China) were transfected into mice at 20 nmol/200 μL via tail injection. Two weeks after the first CCl_4 injection or HFD, mice were injected with AC and ago-miR-455-3p twice a week until the end of CCl_4 and HFD treatment. For BDL, mice were injected with AC and ago-miR-455-3p by tail vein injection after BDL twice a week for 2 weeks. Mice were sacrificed 2 weeks after BDL. Untreated control mice were injected with AC and ago-miR-455-3p by tail vein injection twice a week for 2 weeks. The livers were collected for further analysis.

Microarray Analysis

Total RNAs were isolated from LX-2 (activated by TGF-β1 for 0 and 24 h), respectively, using TRIzol reagent (Life Technologies, Grand Island, NY, USA) and purified using mirVana miRNA Isolation Kit (Life Technologies, Grand Island, NY, USA). Microarray hybridization, scanning, and analysis were performed at Shanghai Biotechnology Corporation (Shanghai, China), and the scanned images were analyzed using Agilent Feature Extraction software (version 10.7).

Flow Cytometric Analysis of Cell Cycle and Apoptosis

Cell Cycle Analysis Kit (Beyotime, Shanghai, China) was utilized to analyze the cell cycle. HSC-T6 and LX-2 cells were digested with trypsin and centrifuged at 1,200 rpm for 5 min. Cells were washed carefully with PBS (twice) and fixed in 70% ethanol prior to storage at −20°C overnight. Before flow cytometry analysis (FCM) detection, the cells were washed twice with PBS, incubated with 50 μg/mL RNase, and stained with propidium iodide (PI) staining solution (500 μL) for 15 min at room temperature for cell-cycle analysis. Apoptotic cells were stained with PI (10 μg/mL; Sigma) and Annexin V-fluorescein isothiocyanate (FITC) (50 μg/mL; BD) in the dark for 15 min at room temperature according to the manufacturer's instructions.

Mouse Liver Fibrosis Induced by BDL, CCl_4, and HFD

Male C57BL/6 mice, 6–8 weeks age, were purchased from Animal Center of Nanjing Medical University (NJMU). All mice were maintained under standard conditions at the animal house of Nanjing Medical University. Experimental hepatic fibrosis was induced by BDL (for 2 weeks) or CCl_4 (10% in olive oil, 2 mL/kg, twice a week for 8 weeks). The hepatic steatosis model was established in mice through feeding an HFD (protein, 18.1%; fat, 61.6%; carbohydrates, 20.3%; D12492; Research Diets, New Brunswick, NJ, USA) continuously for 24 weeks. Mice administered a negative control (NC) diet (protein, 18.3%; fat, 10.2%; carbohydrates, 71.5%; D12450B; Research Diets) served as controls. All animal experiments were performed following a guideline from the Animal Experiment Administration Committee of the university. The animal protocol has been approved by the Institutional Animal Care and Use Committee (IACUC) of Nanjing Medical University.

Masson and Sirius Red Staining

For Masson staining, paraffin-embedded tissue sections were stained with hematoxylin for 1 min and then Masson li Chunhong acid fuchsine solution for 5 min. For Sirius red staining, the formalin-fixed, paraffin-embedded sections were hydrated in distilled water and stained with 0.1% Sirius red for 1 h. After that, the nuclei were counterstained with hematoxylin for 5 min. The slides were dehydrated in 100% ethanol and mounted. The slides were then scanned, and representative images were pictured. The staining was further quantified by a pathologist, and the proportion of the Masson-positive and Sirius red-positive area was calculated.

Cell Viability Assay

For detection of cell viability, HSC-T6 and LX-2 cells were seeded into 96-well plates (2,000 cells/well) and cultured with DMEM (10% FBS) for 5 days. Cell Counting Kit-8 (CCK-8; Dojindo, Kumamoto, Japan) solution (10 μL) was added to each well at the indicated time point, and cells were incubated for 2 h at 37°C. Cell viability was assessed by measurement of the optical density measured at 450 nm.

Immunohistochemical Analysis

Tissue sections were fixed in 4% formalin and then embedded in paraffin. After blocking endogenous peroxides and proteins, sections (thickness, 4 μm) were incubated overnight at 4°C with a prediluted primary antibody of HSF1 or α-SMA (1:500; Cell Signaling Technology). After washing with PBS, sections were incubated with HRP-polymer-conjugated secondary antibody at 37°C for 1 h.

Subsequently, the signal was developed with 3,3′-diaminobenzidine tetrachloride, and the nuclei were counterstained with hematoxylin.

Luciferase Reporter Assay

The 3′ UTR of human HSF1-containing putative binding sites was cloned into the pGL3 plasmid (Ambion, Austin, TX, USA), with the resulting expression vectors being named WT-HSF1-3′ UTR. An altered HSF1 3′ UTR carrying a mutation in the miR-455-3p binding sequence was created and inserted into the pGL3 plasmid, with the resulting construct being named mutant (MUT)-HSF1-3′ UTR. HSC-T6 and LX-2 cells were seeded in 24-well plates (5×10^5 cells/well) and incubated for 24 h before transfection. Cells were co-transfected with 0.12 μg of either pGL3-HSF1-WT or pGL3-HSF1-MUT reporter plasmids together with 40 nM miR-455-3p mimic or negative control oligoribonucleotides using Lipofectamine 3000 (Invitrogen). HSC-T6 and LX-2 cells were also transfected with 0.01 μg of Renilla luciferase expression plasmid as a reference control. HSC-T6 and LX-2 cells were collected after 48 h and lysed using lysis buffer (Promega). The luciferase reporter assay was conducted using the Dual-luciferase Reported Assay System (Promega) according to the manufacturer's instructions.

Statistical Analysis

The statistical analyses were performed using Student's t test (two-tailed) with the Social Sciences (SPSS) software version 19.0. Categorical data were evaluated by the χ^2 test. A value of $p < 0.05$ was considered statistically significant.

AUTHOR CONTRIBUTIONS

S.W. and Q.W. contributed to designing and organizing the experiments, carrying out data analysis, and writing the manuscript. H.Z., J.Q., and C.S. contributed to data analysis. L.L., S.Z., R.L., and C.L. contributed to conceiving the ideas and supervising the study. All authors read and approved the final manuscript.

CONFLICTS OF INTEREST

The authors declare no competing interests.

ACKNOWLEDGMENTS

This study was supported by the National Natural Science Foundation of China (grants 81521004, 1310108001, 81100270, 81210108017, 81600450, and 31700791), National Science Foundation of Jiangsu Province (grants BK20131024 and BE2016766), 863 Young Scientists Special Fund (grant SS2015AA0209322), and the Foundation of Jiangsu Collaborative Innovation Center of Biomedical Functional Materials (to L.L.); The Dumont Research Foundation; and a project funded by the PAPD.

REFERENCES

1. Ma, P.F., Gao, C.C., Yi, J., Zhao, J.L., Liang, S.Q., Zhao, Y., Ye, Y.C., Bai, J., Zheng, Q.J., Dou, K.F., et al. (2017). Cytotherapy with M1-polarized macrophages ameliorates liver fibrosis by modulating immune microenvironment in mice. J. Hepatol. *67*, 770–779.
2. Lodder, J., Denaës, T., Chobert, M.N., Wan, J., El-Benna, J., Pawlotsky, J.M., Lotersztajn, S., and Teixeira-Clerc, F. (2015). Macrophage autophagy protects against liver fibrosis in mice. Autophagy *11*, 1280–1292.
3. Pradere, J.P., Kluwe, J., De Minicis, S., Jiao, J.J., Gwak, G.Y., Dapito, D.H., Jang, M.K., Guenther, N.D., Mederacke, I., Friedman, R., et al. (2013). Hepatic macrophages but not dendritic cells contribute to liver fibrosis by promoting the survival of activated hepatic stellate cells in mice. Hepatology *58*, 1461–1473.
4. Matsuda, M., Tsurusaki, S., Miyata, N., Saijou, E., Okochi, H., Miyajima, A., and Tanaka, M. (2018). Oncostatin M causes liver fibrosis by regulating cooperation between hepatic stellate cells and macrophages in mice. Hepatology *67*, 296–312.
5. Ding, N., Hah, N., Yu, R.T., Sherman, M.H., Benner, C., Leblanc, M., He, M., Liddle, C., Downes, M., and Evans, R.M. (2015). BRD4 is a novel therapeutic target for liver fibrosis. Proc. Natl. Acad. Sci. USA *112*, 15713–15718.
6. Kocabayoglu, P., Lade, A., Lee, Y.A., Dragomir, A.C., Sun, X., Fiel, M.I., Thung, S., Aloman, C., Soriano, P., Hoshida, Y., and Friedman, S.L. (2015). β-PDGF receptor expressed by hepatic stellate cells regulates fibrosis in murine liver injury, but not carcinogenesis. J. Hepatol. *63*, 141–147.
7. Ha, M., and Kim, V.N. (2014). Regulation of microRNA biogenesis. Nat. Rev. Mol. Cell Biol. *15*, 509–524.
8. Zhou, L., Liu, S., Han, M., Ma, Y., Feng, S., Zhao, J., Lu, H., Yuan, X., and Cheng, J. (2018). miR-185 Inhibits Fibrogenic Activation of Hepatic Stellate Cells and Prevents Liver Fibrosis. Mol. Ther. Nucleic Acids *10*, 91–102.
9. Mogler, C., Wieland, M., König, C., Hu, J., Runge, A., Korn, C., Besemfelder, E., Breitkopf-Heinlein, K., Komljenovic, D., Dooley, S., et al. (2015). Hepatic stellate cell-expressed endosialin balances fibrogenesis and hepatocyte proliferation during liver damage. EMBO Mol. Med. *7*, 332–338.
10. Chen, J., Yu, Y., Li, S., Liu, Y., Zhou, S., Cao, S., Yin, J., and Li, G. (2017). MicroRNA-30a ameliorates hepatic fibrosis by inhibiting Beclin1-mediated autophagy. J. Cell. Mol. Med. *21*, 3679–3692.
11. Li, J., Ghazwani, M., Zhang, Y., Lu, J., Li, J., Fan, J., Gandhi, C.R., and Li, S. (2013). miR-122 regulates collagen production via targeting hepatic stellate cells and suppressing P4HA1 expression. J. Hepatol. *58*, 522–528.
12. Ma, L., Yang, X., Wei, R., Ye, T., Zhou, J.K., Wen, M., Men, R., Li, P., Dong, B., Liu, L., et al. (2018). MicroRNA-214 promotes hepatic stellate cell activation and liver fibrosis by suppressing Sufu expression. Cell Death Dis. *9*, 718.
13. Borberg, H. (2013). The lower the better: target values after LDL-Apheresis and semi-selective LDL-elimination therapies. Transfus. Apheresis Sci. *48*, 203–206.
14. Bataller, R., and Brenner, D.A. (2005). Liver fibrosis. J. Clin. Invest. *115*, 209–218.
15. Miura, K., Kodama, Y., Inokuchi, S., Schnabl, B., Aoyama, T., Ohnishi, H., Olefsky, J.M., Brenner, D.A., and Seki, E. (2010). Toll-like receptor 9 promotes steatohepatitis by induction of interleukin-1beta in mice. Gastroenterology *139*, 323–334.e7.
16. Xu, M.Y., Hu, J.J., Shen, J., Wang, M.L., Zhang, Q.Q., Qu, Y., and Lu, L.G. (2014). Stat3 signaling activation crosslinking of TGF-β1 in hepatic stellate cell exacerbates liver injury and fibrosis. Biochim. Biophys. Acta *1842*, 2237–2245.
17. Yang, J.J., Tao, H., Hu, W., Liu, L.P., Shi, K.H., Deng, Z.Y., and Li, J. (2014). MicroRNA-200a controls Nrf2 activation by target Keap1 in hepatic stellate cell proliferation and fibrosis. Cell. Signal. *26*, 2381–2389.
18. Calvopina, D.A., Chatfield, M.D., Weis, A., Coleman, M.A., Fernandez-Rojo, M.A., Noble, C., Ramm, L.E., Leung, D.H., Lewindon, P.J., and Ramm, G.A. (2018). MicroRNA Sequencing Identifies a Serum MicroRNA Panel, Which Combined With Aspartate Aminotransferase to Platelet Ratio Index Can Detect and Monitor Liver Disease in Pediatric Cystic Fibrosis. Hepatology *68*, 2301–2316.
19. Yang, H., Wei, Y.N., Zhou, J., Hao, T.T., and Liu, X.L. (2017). MiR-455-3p acts as a prognostic marker and inhibits the proliferation and invasion of esophageal squamous cell carcinoma by targeting FAM83F. Eur. Rev. Med. Pharmacol. Sci. *21*, 3200–3206.
20. Singh, A.K., Rooge, S.B., Varshney, A., Vasudevan, M., Bhardwaj, A., Venugopal, S.K., Trehanpati, N., Kumar, M., Geffers, R., Kumar, V., and Sarin, S.K. (2018). Global microRNA expression profiling in the liver biopsies of hepatitis B virus-infected patients suggests specific microRNA signatures for viral persistence and hepatocellular injury. Hepatology *67*, 1695–1709.

21. Zhou, Y., Lv, X., Qu, H., Zhao, K., Fu, L., Zhu, L., Ye, G., and Guo, J. (2018). Preliminary screening and functional analysis of circular RNAs associated with hepatic stellate cell activation. Gene *677*, 317–323.

22. McArdle, A., Pollock, N., Staunton, C.A., and Jackson, M.J. (2019). Aberrant redox signalling and stress response in age-related muscle decline: role in inter- and intra-cellular signalling. Free Radic. Biol. Med. *132*, 50–57.

23. Barna, J., Csermely, P., and Vellai, T. (2018). Roles of heat shock factor 1 beyond the heat shock response. Cell. Mol. Life Sci. *75*, 2897–2916.

24. Akerfelt, M., Morimoto, R.I., and Sistonen, L. (2010). Heat shock factors: integrators of cell stress, development and lifespan. Nat. Rev. Mol. Cell Biol. *11*, 545–555.

25. Hetz, C. (2012). The unfolded protein response: controlling cell fate decisions under ER stress and beyond. Nat. Rev. Mol. Cell Biol. *13*, 89–102.

26. Wu, J., Liu, J., Ding, Y., Zhu, M., Lu, K., Zhou, J., Xie, X., Xu, Y., Shen, X., Chen, Y., et al. (2018). MiR-455-3p suppresses renal fibrosis through repression of ROCK2 expression in diabetic nephropathy. Biochem. Biophys. Res. Commun. *503*, 977–983.

27. Gomez-Pastor, R., Burchfiel, E.T., and Thiele, D.J. (2018). Regulation of heat shock transcription factors and their roles in physiology and disease. Nat. Rev. Mol. Cell Biol. *19*, 4–19.

28. Ikejima, K., Honda, H., Yoshikawa, M., Hirose, M., Kitamura, T., Takei, Y., and Sato, N. (2001). Leptin augments inflammatory and profibrogenic responses in the murine liver induced by hepatotoxic chemicals. Hepatology *34*, 288–297.

29. Park, S.J., Sohn, H.Y., and Park, S.I. (2013). TRAIL regulates collagen production through HSF1-dependent Hsp47 expression in activated hepatic stellate cells. Cell. Signal. *25*, 1635–1643.

30. Ito, S., and Nagata, K. (2017). Biology of Hsp47 (Serpin H1), a collagen-specific molecular chaperone. Semin. Cell Dev. Biol. *62*, 142–151.

31. Jiang, X., Zhou, T., Wang, Z., Qi, B., and Xia, H. (2017). HSP47 Promotes Glioblastoma Stemlike Cell Survival by Modulating Tumor Microenvironment Extracellular Matrix through TGF-β Pathway. ACS Chem. Neurosci. *8*, 128–134.

32. Borges, F.T., Melo, S.A., Özdemir, B.C., Kato, N., Revuelta, I., Miller, C.A., Gattone, V.H., 2nd, LeBleu, V.S., and Kalluri, R. (2013). TGF-β1-containing exosomes from injured epithelial cells activate fibroblasts to initiate tissue regenerative responses and fibrosis. J. Am. Soc. Nephrol. *24*, 385–392.

33. Perumal, N., Perumal, M., Halagowder, D., and Sivasithamparam, N. (2017). Morin attenuates diethylnitrosamine-induced rat liver fibrosis and hepatic stellate cell activation by co-ordinated regulation of Hippo/Yap and TGF-β1/Smad signaling. Biochimie *140*, 10–19.

34. Sulaiman, A.A., Zolnierczyk, K., Japa, O., Owen, J.P., Maddison, B.C., Emes, R.D., Hodgkinson, J.E., Gough, K.C., and Flynn, R.J. (2016). A Trematode Parasite Derived Growth Factor Binds and Exerts Influences on Host Immune Functions via Host Cytokine Receptor Complexes. PLoS Pathog. *12*, e1005991.

35. Shen, H., and Wang, Y. (2019). Activation of TGF-β1/Smad3 signaling pathway inhibits the development of ovarian follicle in polycystic ovary syndrome by promoting apoptosis of granulosa cells. J. Cell. Physiol. *234*, 11976–11985.

36. Xu, F., Liu, C., Zhou, D., and Zhang, L. (2016). TGF-β/SMAD Pathway and Its Regulation in Hepatic Fibrosis. J. Histochem. Cytochem. *64*, 157–167.